URSI GASS 2020, Rome, Italy, 29 August - 5 September 2020

Electromagnetic Modeling and Correction of RFID Temperature Sensors under Random Wireless Interrogation

Francesca Camera*(1), and Gaetano Marrocco(1)
(1) Pervasive Electromagnetics Lab, University of Roma Tor Vergata, www.pervasive.ing.uniroma2.it. Corresponding author: gaetano.marrocco@uniroma2.it.

Abstract

UHF-Radio frequency identification (RFID) technology applied for sensing procedures is nowadays a well-established trend. However, the response of the Integrated Circuit (IC) transponder is sensitive to the strength of the interrogating power that may produce non linear effects and alterations in measurement evaluation. Starting from experimental measurements on tags with integrated temperature sensor, this work demonstrates that the error affecting the measurement is, in some conditions, predictable and hence correctable. An electromagnetic-thermal correction model is proposed and validated, with the final aim to overcome the instabilities due to the chip non-linearity.

1 Introduction

Wearable devices for the remote real-time monitoring of human physiological signals for health-related purposes is a growing field in application-oriented research [1, 2, 3]. The current evolution of wearable devices is toward the *Epidermal Electronics* [4], where electronic components for sensing and data transmission are deployed onto a thin and flexible membrane directly attached onto the skin like a thin plaster or a tattoo. Battery-less radio frequency identification (RFID) technology fits very well with the requirements of low-cost, wireless communication and user's comfort.
Among all the biophysical parameters that can be collected with RFID sensors, body temperature is one of the most effective biometric indicators revealing the health condition of a person and it is normally monitored in both hospital and domestic environments. Thermometers for body temperature monitoring requires an accuracy less or equal to ± 0.25 °C [5].
Unfortunately, it is well-known that the response of the Integrated Circuit (IC) transponder is sensitive to the strength of the impinging power that may produce non-linear effects on IC responses [6, 7]. In particular, fictitious alteration in the measured skin temperature was found in [8] with an EM4325 IC [9] when changing the mutual reader-to-tag distance. In particular, an anomalous and not reliable increase up to more than 1 °C was found when the reader was very close (less than 1 cm) to the tag. The authors proposed to eliminate all the measurements obtained when the instantaneous backscattered power was higher than a threshold derived experimentally. However, the backscattered power collected by the reader is not an IC specific parameter as it mainly depends on the propagation channel and, hence, it can not be considered a robust metric in real conditions.
The recently introduced family of RFID ICs for temperature measurement also returns indication on the electromagnetic power (denoted as *Power on Chip*) delivered to the IC itself [10], so they open new opportunities for data conditioning. Manufacturers suggest that the temperature measurement has to be considered of good accuracy when the returned Power on Chip is within a given narrow range. Although this tool greatly improve the reliability of the measurement, the requested condition is rather stringent. The demand for an accurate control of the measurement conditions is indeed not easy to be accomplished neither through of an hand-held device, used by a common operator (like nurses in hospital monitoring), nor by a fixed reader when the user is in motion.
In this work the authors introduce an electromagnetic-thermal model for UHF-RFID (860-960 MHz) temperature oriented ICs that is used to make the temperature reading nearly insensitive to the reading modality. The leading idea is to correct the temperature samples, even outside the safe power on chip range that is declared by the manufacturer, by means of a first order model that relates the power on chip to the induced disturb on the temperature data. The correction parameters are evaluated by means of experimentation and data fitting on a set of tags in controlled conditions and hence applied to another tag not belonging to the set used for data fitting. The overall result is that most of the measured samples are meaningful and there is no need to discard some data. The expected benefit is a quicker and more robust measurement procedure.

2 Problem formulation and Correction Model

It is known that the analog response of the IC, including the input impedance, the power sensitivity and also the measured temperature, are not insensitive to the power on chip P_{IC} that is collected by the tag antenna, following the interrogation by the reader, and finally delivered to the IC [3]:

$$P_{IC} = \left(\frac{\lambda_0}{4\pi d}\right)^2 P_{in} G_R(\theta,\varphi)\hat{G}_T(\theta,\varphi)\chi(\theta,\varphi) \qquad (1)$$

where, a free-space link [1] is assumed for the sake of simplicity.
Experience indicates that the rise of the interrogation power induces an increase of the measured temperature T_{IC} (so $T_{IC}[P_{IC}]$) while the decrease of that power produces an intensification of the standard deviation $\sigma_T[P_{IC}]$, thus making the measurements less precise.
It is here postulated that the disturbing effect on the temperature produced by the variable power on-chip in the range

$$p_1 \leq P_{IC} \leq p_2 \tag{2}$$

can be accounted for by a linear relationship. Bounds p_1,p_2 are generally dependent on the IC family and, in particular, the lower bound p_1 is the minimum power on chip for which the returned temperature data exhibits a standard deviation smaller than an acceptable value $\sigma_{T,max}$. The temperature returned by the wireless sensor is then written as:

$$T_{IC}[P_{IC}] = T_{RFID}[P_{IC,0}](T) + \alpha[P_{IC}] \tag{3}$$

where $P_{IC,0} \in (p_1, p_2)$ is a reference value of the power on chip for which the IC has been calibrated, so that $T_{RFID}[P_{IC,0}](T)$ is the artifact-free temperature measure corresponding to that power. The function α, parametrizing the artifact, is expressed as:

$$\alpha[P_{IC}] = a \cdot (P_{IC} - P_{IC,0}) + b \tag{4}$$

The artifact can be else removed by inverting (3) so that the corrected temperature will be:

$$T_{RFID}(T) = T_{IC}[P_{IC}](T) - \alpha[P_{IC}] \tag{5}$$

The parameters a and b of the artifact can be estimated by means of a linear regression of the response of a test population of N tags that are evaluated at the fixed reference temperature T_{ref}. ICs are hence assumed to be calibrated at T_{ref} for $P_{IC} = P_{IC,0}$ so that, after averaging on M samples, $\overline{T}_{RFID}[P_{IC,0}](T_{ref}) = T_{ref} \pm \sigma_T$.
At this purpose, during a measurement at fixed temperature, the power emitted by the reader is linearly increased so that the power on chip spans in the useful range $p_1 \leq P_{IC} \leq p_2$ and the temperature of the nth tag is stored. The procedure is repeated for each n=1...N tag. Then, parameters $\{a, b\}$ are evaluated by enforcing the linear regression based on the collected data for all the N test tags:

$$T_{IC,n}[P_{IC,n}] - T_{IC,n}[P_{IC,0,n}] \rightarrow a(P_{IC} - P_{IC,0}) + b \tag{6}$$

The above procedure is demonstrated in the next paragraph by means of COTS temperature sensing tags.

[1] λ_0 is the free-space wavelength of the carrier tone emitted by the reader; θ, φ are the angles of a spherical coordinate system centered at the tag; P_{in} is the power entering the reader's antenna; $G_R(\theta,\varphi)$ is the gain of the reader antenna; χ is the polarization factor accounting for the mutual orientation reader-tag; $\hat{G}_T(\theta,\varphi) = G_T(\theta,\varphi)\cdot\tau$ is the realized gain of the tag, e.g. the radiation gain $G_T(\theta,\varphi)$ of the antenna corrected by the power transfer coefficient τ between tag's antenna and microchip.

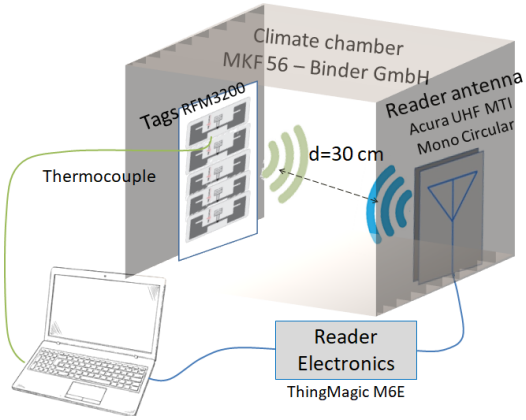

Figure 1. Measurement setup for estimation of correction parameters comprising a climate chamber kept at a fixed temperature

3 Experimental analysis with COTS Tags

3.1 The Sensor-oriented RFID IC

The RFID IC that will be hereafter used in the experimental analysis is the Axzon Magnus® S3 that provides temperature samples in the range -40 °C to +85 °C with a resolution of 0.13 °C. According to the manufacturer, these tags are two-points calibrated at 24.6 °C and 80 °C. This IC is moreover capable to return a measure of the instantaneous power-on-chip P_{IC} through a 5bit word (0-31), denoted $RSSI$[2] *on chip* (hereafter $RSSI_C$). All the discussions in the previous Section will be then referred to $RSSI_C$ instead of P_{IC}. It is worth mentioning that the IC datasheet suggests that reliable temperature data are achieved only for the very narrow range $13 \leq RSSI_C \leq 18$. Accordingly, it will be hereafter considered as reference a power on chip value of $RSSI_{C,0} = 17$ (for which the IC has been calibrated and so the tag response is reasonable assumed as artifact-free). The proposed procedure will demonstrate the ability of the correction to sensibly extend the $RSSI_C$ range.

3.2 Measurement Set-up

The test population for the estimation of the correction parameters is composed of four RFM3200 dipole tags for general purpose applications. Test tags were placed inside a climate chamber (MKF 56 - Binder GmbH) [11] to perform measurements at stable temperature $T = 36 \pm 0.1$°C and powered at two different frequencies: 867 MHz (ETSI Band) and 915 MHz (FCC Band). A calibrated thermocouple probe was attached close to the tags to measure the *true* temperature.

The ThingMagic M6E RFID reader was connected to Acura UHF Antenna MTI Mono Circular [12] inside the climatic chamber in broadside direction at a distance of 30 cm from the tag under test (Fig.1). The five tags were inde-

[2] Receiver Signal Strength Indication

pendently interrogated one by one with a sampling rate of 3 Hz.

3.3 Computation of the Correction Parameters

During each tag interrogation, the reader was fed with increasing input power profile such that the resulting $RSSI_C$ was a stepwise function within $3 \leq RSSI_C \leq 31$ with time steps of 60 s that corresponds to 180 temperature samples for each fixed power. In spite of the nearly stable temperature outcome of a reference thermocouple, RFID temperature exhibits a remarkable drift when the strength of the power on chip increases. A larger dispersion of the collected data is instead evident for $RSSI_C < 10$.
The error

$$\Delta T_n(RSSI_C) = T_{IC,n}[RSSI_C] - < T_{IC,n}[RSSI_{C,0}] > \qquad (7)$$

due to the power on-chip artifacts versus the $RSSI_C - RSSI_{C,0}$ is shown in Fig.2. It is worth noting that $RSSI_C = 31$ (i.e. $RSSI_C - RSSI_{C,0} = 14$) is the upper bound that the IC is capable to return. This means that if the P_{IC} increases, the $RSSI_C$ saturates and becomes insensitive to the strength of the impinging power that, however, induces artifacts in measurements. For this reason, $RSSI_C = 31$ can not be used in (6) to obtain the correction coefficient. Mean $\sigma_T[RSSI_C - RSSI_{C,0}]$ remains below 0.25 ° C when $RSSI_C \geq 12$ (i.e. $RSSI_C - RSSI_{C,0} \geq -5$). So, by applying the linear regression to the whole set of data for $12 \leq RSSI_C \leq 30$, the resulting correction coefficients are $a = 0.09$; $b = 0$. After correction, the error in (7) is mitigated as in Fig.3 and the resulting averaged accuracy in that $RSSI_C$ range is ± 0.06 °C, that is less than the resolution of the IC sensor itself. Accordingly, the proposed power correction method has extended the usability of the sensor for most of the $RSSI_C$ dynamic range.

4 Correction Model Validation

4.1 Measurement set-up

The power based correction procedure proposed above is now applied to the measurement of temperature by means of another tag that embeds the same IC as before. The tag was placed inside the climate chamber where the temperature was kept fixed at 36 °C.
A thermocouple was also placed together with the tag as a reference. The output radiated power was raised stepwise as before, so that each step lasted one minute. Raw measurements are then corrected in post-processing according to the procedure described in Section 2, i.e.: i) data corresponding to $RSSI_C < 12$ and $RSSI_C = 31$ were discarded; ii) the remaining useful samples were then linearly corrected by means of the the parameters a and b obtained above; iii) a moving average with a 10-samples window was finally applied to remove dispersion.

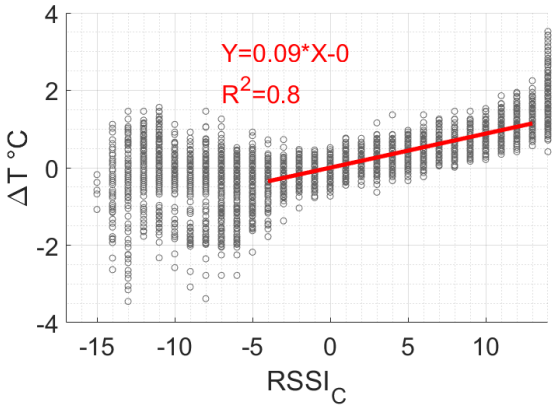

Figure 2. Error of the temperatures $T_{IC,n}[RSSI_C]$ transmitted back by the four sensors during the step-wise increase of the power on-chip, with respect to the average temperature, $< T_{IC,n}[RSSI_{C,0}] >$, corresponding to the reference power $RSSI_{C,0} = 17$ used to calibrate the ICs. Superimposed, the linear regression for $12 \leq RSSI_C \leq 30$ to extract the correction parameters a, b.

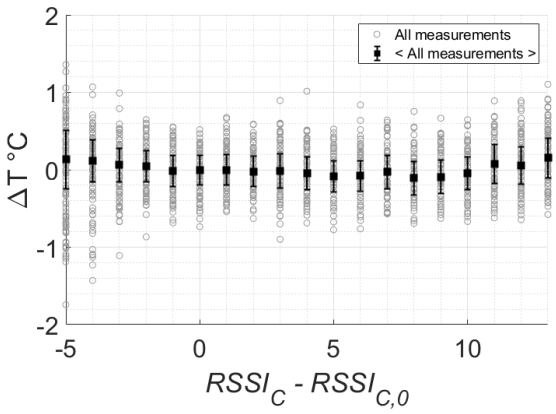

Figure 3. Error in each measurement from Fig.2 after correction, and averaging.

4.2 Results

As expected, the variable power produces a relevant change of the temperature returned by the IC. Fig.4 shows that, compared with the temperature returned by the thermocouple, measurements without correction deviate from *true* temperature even by 1 °C, thus returning, for example, a false fever indication. By applying the power based correction, the RFID data become less sensitive to the $RSSI_C$ values and the maximum error vs. the thermocouple is reduced to 0.2 °C.

5 Conclusion

The effects on temperature measurement related to power distortion have been deepened for RF-Micron IC tags. Starting from experimental measurements on four different

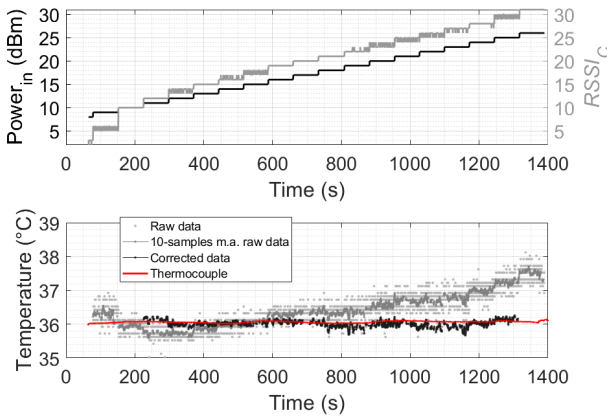

Figure 4. a) Stepwise increasing input power and $RSSI_C$ recorded by IC; b) Temperature measurement and comparison between raw data without (grey dots and line) and with (black) correction.

tags at two fixed frequencies varying the $RSSI_c$, the temperature shift due to $RSSI_c$ variation has been evaluated. This temperature shift is, for some conditions, predictable and so correctable. This effect permits to extend the $RSSI_c$ range of measurement reliability maintaining an acceptable accuracy and to establish a reading protocol in order to overcome the instabilities due to the chip non-linearity.

6 Acknowledgements

Work funded by Lazio Innova, project SECOND SKIN. Ref. 85-2017-14774.

References

[1] S. C. Mukhopadhyay, "Wearable sensors for human activity monitoring: A review," *IEEE sensors journal*, vol. 15, no. 3, pp. 1321–1330, 2014.

[2] K. Guk, G. Han, J. Lim, K. Jeong, T. Kang, E.-K. Lim, and J. Jung, "Evolution of wearable devices with real-time disease monitoring for personalized healthcare," *Nanomaterials*, vol. 9, no. 6, p. 813, 2019.

[3] Y. Lee, M. Mahmood, Y.-S. Kim, R. W. Hafenstine, and W.-H. Yeo, "Multifunctional wearable biopatch for real-time monitoring of physiological activities," in *Nano-, Bio-, Info-Tech Sensors and 3D Systems III*, vol. 10969. International Society for Optics and Photonics, 2019, p. 1096907.

[4] J. A. Rogers, R. Ghaffari, and D.-H. Kim, *Stretchable bioelectronics for medical devices and systems*. Springer, 2016.

[5] J. Rubia-Rubia, A. Arias, A. Sierra, and A. Aguirre-Jaime, "Measurement of body temperature in adult patients: comparative study of accuracy, reliability and validity of different devices," *International journal of nursing studies*, vol. 48, no. 7, pp. 872–880, 2011.

[6] G. A. Vera, Y. Duroc, and S. Tedjini, "Rfid test platform: Nonlinear characterization," *IEEE Transactions on Instrumentation and Measurement*, vol. 63, no. 9, pp. 2299–2305, 2014.

[7] M. C. Caccami and G. Marrocco, "Electromagnetic modeling of self-tuning rfid sensor antennas in linear and nonlinear regimes," *IEEE Transactions on Antennas and Propagation*, vol. 66, no. 6, pp. 2779–2787, 2018.

[8] C. Miozzi, S. Amendola, A. Bergamini, and G. Marrocco, "Clinical trial of wireless epidermal temperature sensors: preliminary results," in *EMBEC & NBC 2017*. Springer, 2017, pp. 1041–1044.

[9] EM4325. Accessed: 2019-12-10. [Online]. Available: https://www.emmicroelectronic.com/product/epc-and-uhf-ics/em4325/

[10] Axzon. RFM3300-E Magnus-S3 M3E passive sensor IC. Accessed: 2019-07-16. [Online]. Available: https://axzon.com/rfm3300-d-magnus-s3-m3d-passive-sensor-ic/

[11] Binder. Accessed: 2020-02-10. [Online]. Available: https://www.binder-world.com/en/products/dynamic-climate-chambers/series-mkf/mkf-56

[12] Acura. Accessed: 2020-02-10. [Online]. Available: http://www.acura.com.br/en-us/products/rfid-antenna/item/antena-monoestatica-7-dbi